One-dimensional nonequilibrium kinetic Ising models with local spin symmetry breaking: *N*-component branching annihilating random-walk transition at zero branching rate

Nóra Menyhárd
Research Institute for Solid State Physics and Optics, P.O. Box 49, H-1525 Budapest, Hungary

Géza Ódor
Research Institute for Technical Physics and Materials Science, P.O. Box 49, H-1525 Budapest, Hungary
(Received 29 March 2002; published 26 July 2002)

The effects of locally broken spin symmetry are investigated in one-dimensional nonequilibrium kinetic Ising systems via computer simulations and cluster-mean-field calculations. Besides a line of directed percolation transitions, a line of transitions belonging to *N*-component, two-offspring branching annihilating random-walk class (*N*-BARW2) is revealed in the phase diagram at zero branching rate. In this way a spin model for *N*-BARW2 transitions is proposed.

DOI: 10.1103/PhysRevE.66.016127 PACS number(s): 05.70.Ln, 82.20.Wt

I. INTRODUCTION

The Ising model is a well-known static equilibrium model. Its dynamical generalizations, the kinetic Ising models, were originally intended to study relaxational processes near equilibrium states [1,2]. Glauber introduced the single spin-flip kinetic Ising model, while Kawasaki constructed a spin-exchange version for studying the case of conserved magnetization. Nonequilibrium kinetic Ising models, in which the steady state is produced by kinetic processes in connection with heat baths at different temperatures, have been widely investigated and results have shown that various phase transitions are possible under nonequilibrium conditions, even in one dimension (1D) (for a review see the article by Rácz in Ref. [3]). Most of these studies, however, have been concerned with the effects the nonequilibrium nature of the dynamics might exert on phase transitions *driven by temperature*.

A different line of investigating nonequilibrium phase transitions has been via branching annihilating random walk (BARW) processes. The parity conservation of particles is decisive in determining the universality class of the phase transition. A coherent picture of this scenario is provided from a renormalization point of view in Ref. [4]. The first example of a BARW model with an even number of offsprings exhibiting the so-called PC (parity conserving) transition was reported by Grassberger *et al.* [5].

A class of general nonequilibrium kinetic Ising models (NEKIM) with combined spin-flip dynamics at $T=0$ and Kawasaki spin-exchange dynamics at $T=\infty$ has been proposed by one of the authors [6] in which, for a range of parameters of the model, PC-type transition takes place. This model has turned out to be very rich in several respects, for a review see Ref. [7].

Absorbing transitions have been, however, mostly studied in particle-type models. The *N*-BARW2 model is a classical stochastic system of *N* types of particles with branching annihilating random walk and two offsprings. For $N=1$ the model exhibits, at finite branching rate *p*, PC-type transition [8–14]. For $N>1$, *N* types of particles A_i perform diffusion, pairwise annihilation of the same species and branching $A_i \to A_i + 2A_j$ with rate *p* for $i=j$ and with rate $p/(N-1)$ for $i \neq j$. In case of $p=0$ this model is always active except for the annihilation fixed point at zero branching rate. According to field theory [4] the coarse-grained, bosonic version of the model forms a different universality class, the so-called *N*-BARW2 with exponents in one dimension as follows: $\nu_\perp=1$, $z=2$, $\alpha=1/2$, $\beta=1$. Here the exponents are defined as follows:

$$\xi \sim p^{-\nu_\perp}, \tau \sim \xi^z, \tag{1}$$

$$\rho(t) \sim t^{-\alpha}, \rho_\infty \sim p^\beta, \tag{2}$$

where τ is the characteristic time, ξ is the correlation length, and $\rho(t)$, ρ_∞ are the particle densities at time *t* and in the steady state, respectively.

Hard core interactions have proven to be relevant in case of the *N*-BARW2 model by drastically changing the universality class [17,18]. The arrangement of the offsprings relative to the parent turns out to be a relevant factor and causes two robust classes that are insensitive to the parity conservation [19] or to the binary nature of the production process [20].

In this paper, we present an asymmetric spin model, NEKIMA, with asymmetry both in the annihilation and spin-flip rate as a generalization of NEKIM. On the level of kinks, however, this model corresponds to a process of *A* and *B* particles with $A \to ABA$- and $B \to BAB$-type branching and $AB \to 0$ annihilation and $BA \to BA$ exclusion. Nevertheless, as will be presented below using computer simulations, the critical properties near the zero branching limit are the same as for the *N*-BARW2 model cited above with no sign of exclusion effects since alternating sequences of *A*'s and *B*'s occur like in Ref. [21], hence hard core interactions cannot play an important role. Moreover, at finite branching rate of the kinks a line of directed percolation (DP) -type transition [15] occurs, which is well described by $N=6$ level cluster-mean-field calculations.

II. THE MODEL

The general form of the Glauber spin-flip transition rate in one dimension for spin s_i sitting at site i is [1] ($s_i = \pm 1$):

$$w(s_i, s_{i-1}, s_{i+1}) = \frac{\Gamma}{2}(1 + \delta s_{i-1} s_{i+1}) \times \left[1 - \frac{1}{2} s_i (s_{i-1} + s_{i+1})\right] \quad (3)$$

at zero temperature. Usually the Glauber model is understood as the special case $\delta = 0$, $\Gamma = 1$.

The Kawasaki spin-exchange transition rate of neighboring spins [2] at $T = \infty$ reduces to an unconditional nearest neighbor exchange:

$$w_{ex}(s_i, s_{i+1}) = \frac{p_{ex}}{2}(1 - s_i s_{i+1}), \quad (4)$$

where p_{ex} is the probability of spin exchange. The quantities in Eqs. (3) and (4) conserve spin symmetry, of course. Concerning spin exchanges, which act only at domain boundaries, the process of main importance here is that a kink can produce two offsprings at the next time step with probability

$$p_{k \to 3k} \propto p_{ex}. \quad (5)$$

By changing p_{ex} for *negative values of* δ this model displays phase transitions in the parity conserving universality class [6].

In the following, we will be interested in investigating an extended version of the above model. Instead of Eq. (3) we will prescribe the rates for the case $\Gamma = 1$, $\delta = 0$ as follows. The $+++ \to +++$ and $--- \to ---$ processes remain as in Eq. (3) i.e., at zero temperature no kink-pair creations occur inside of domains. Further rates will be chosen in such a way that they break the symmetry of $+$ and $-$ spins locally. Such dynamically self-induced field was first investigated in a different context by Majumdar, Dean, and Grassberger (MDG) [16], namely, in studying the $T = 0$ coarsening dynamics of an Ising chain in a local field, which favors $-$ spins as compared to $+$ ones dynamically.

In addition to the choice in Ref. [16] concerning the asymmetry in the annihilation rate

$$w(+;--) = 1, \quad (6)$$

$$w(-;++) = 0, \quad (7)$$

further spin symmetry breaking will be introduced here, namely, in the spin-flip part of the Glauber transition rate the strength of which will be measured by a further parameter p_+. While the transition rate

$$w(-;+-) = w(-;-+) = 1/2 \quad (8)$$

is unchanged, the two rates flipping $+$ spins will be reduced as

$$w(+;+-) = w(+;-+) = p_+ < 1/2 \quad (9)$$

in order to balance the effect of the other dynamically induced field arising from Eqs. (6) and (7) by locally favoring $+$ spins. The spin-exchange part of the model remains as in the spin-symmetric case (4).

In the terminology of domain walls or particles, the following reaction-diffusion picture arises. There are two kinds of domain walls: $-+ \equiv A$ and $+- \equiv B$, which can only occur alternately because of the spin background. Upon meeting $AB \to 0$ while in the opposite sequence BA, the two domain walls are repulsive due to Eq. (7).

The absorbing states in the extreme situation $p_+ = 0$ when spin flipping maximally favors $+$ spins, are states with single frozen $-$ spins such as $+-+++-++-+++$. By increasing p_+, a slow random walk of these lonely $-$ spins starts and by annihilating random walk only one of them survives and performs RW. The all $+$ and all $-$ states are, of course, also absorbing.

The inclusion of nearest neighbor spin exchange (4) changes the picture drastically. Spin exchange leads to $A \to ABA$- and $B \to BAB$-type kink production, which together with $AB \to 0$ annihilation [$BA \to 0$ is forbidden due to the annihilation asymmetry, Eqs. (6) and (7)] and diffusion of A and B leads to a kind of two-component, coupled branching and annihilating random walk. The phase diagram and the nature of the transitions will be reported and discussed in the following.

III. PHASE DIAGRAM OF THE NEKIMA MODEL

A. The line of DP transitions

1. Simulation results

Given three independent parameters δ, p_+, and p_{ex} (or rather p_{ex}/Γ) with the restriction, Eq. (9), it is hard to explore the whole phase diagram. In the original (spin-symmetric) case of NEKIM [6], we have investigated the phase boundary in the parameter space (δ, p_{ex}). For *negative* values of δ a line of PC transitions was found. We are not going to investigate the $\delta < 0$ case in the following and only make the remark that spin asymmetry as introduced above (with a trivial generalization for $\delta < 0$), changes the parity conserving character of the transitions to directed percolation type (of two species), as could be expected. The case $\delta \geqslant 0$ (including the Glauber case $\Gamma = 1, \delta = 0$) was found to be Ising-like, for all values of p_{ex}.

Introducing spin asymmetry, however, makes the Glauber case also richer in phases. The phase diagram in the plane of parameters p_{ex} and $p_+ < 1/2$ as obtained by computer simulations is shown in Fig. 1.

In fixing the phase boundary the quantity measured was the density of kinks $\rho(t)$ as a function of time starting from a random initial distribution of up and down spins. The chain size L varied between $L = 2000$–5000 and up to $t = 5 \times 10^5$ Monte Carlo steps (MCS) were reached. The way of updating was as in Ref. [6]. A line of DP transitions has been found by the power-law behavior of $\rho(t) \sim t^{-\alpha}$ with $\alpha = 0.160 \pm 0.005$, the value characteristic of DP transition. This was, of course, the expected kind of order-disorder transition on the basis of spin asymmetry.

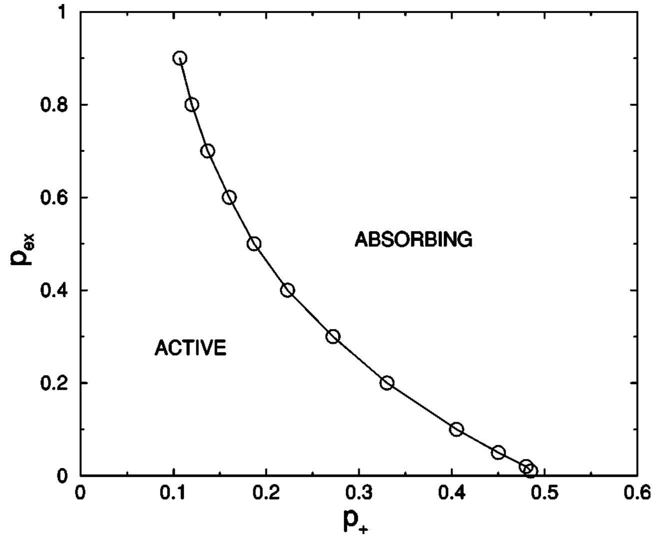

FIG. 1. Phase diagram of the NEKIMA model for $\delta=0$, $\Gamma=1$. The absorbing (fully $-$) phase lies above the boundary. The $p_+=0.5$ point is referred to as the MDG point in the text.

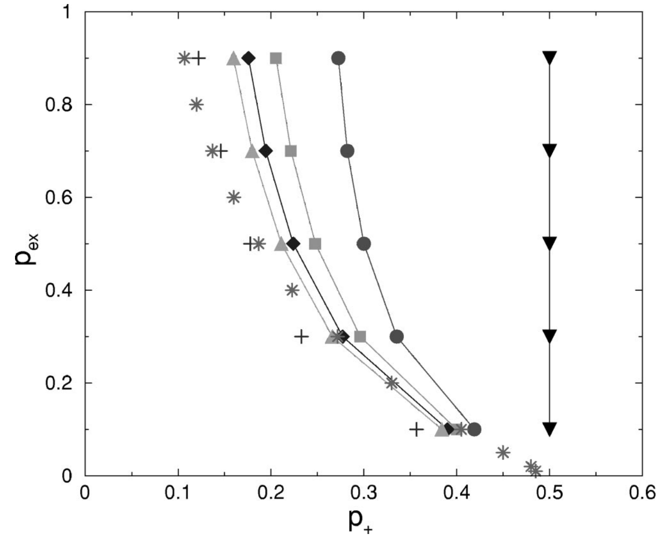

FIG. 2. Phase diagram determined by $N=2-6$ cluster-mean-field approximations (filled symbols from right to left), the $N\to\infty$ extrapolated values (plus signs) and simulation results (stars).

The point $p_+=1/2$, $p_{ex}=0$ is a particular one, at this point our model goes over to the one investigated by Majumdar *et al.* [16]. For these parameter values a very high precision computer measurement has given the result $\rho(t)=t^{-1/2}/\ln(t/\tau)$ supporting an analytic independent interval approximation by these authors. In an equivalent model, however, the deviation from the $t^{-1/2}$ law has shown up as an initial density-dependent power function with a power of $\rho(t)$ slightly deviating from 1/2 [22]. This problem, however, is not the subject of the present investigation.

Concerning the phase diagram, Fig. 1, the parameter values in the vicinity of $p_+=1/2$ for $p_{ex}\neq 0$ are hard from the computational point of view as long transients show up in the time evolution. It is apparent, however, that the phase line ends up here tangentially. At $p_+=1/2$ the effect of the exchange term is such that for all $p_{ex}>0$ the absorbing phase is entered: due to the choice in Eqs. (6) and (7), the all $s_i=-1$ phase (one of the absorbing phases) is reached exponentially fast.

As to the other limiting situation $p_+=0$, for $p_{ex}=0$ the initial spin distribution freezes in. As a matter of fact, the line of phase transitions reaches the $p_+=0$ axis only by letting $p_{ex}/\Gamma\to\infty$ by $\Gamma\to 0$ [Γ is only fixing the rate of flips, see Eq. (3), while here we fixed it to unity]. This circumstance, however, is of no importance for the results.

2. Cluster-mean-field calculations for the phase diagram

Cluster-mean-field approximation introduced for nonequilibrium models by Refs. [23,24] was applied for the present model. The $N=1$ mean-field equation for spin-up density is

$$\frac{\partial\rho_1}{\partial t}=-2p_+(1-\rho_1)\rho_1^2, \qquad (10)$$

which independently from p_{ex} gives a $\rho_1\propto t^{-1}$ leading order decay to the $\rho_1(\infty)=0$ solution for all $p_+>=0$, while it is constant (keeps the initial value) for $p_+=0$. Therefore, this predicts a discontinuous transition along the $p_+=0$ axis. The corresponding steady state exponent is $\beta=0$. Similarly the kink density, $\rho_1(1-\rho_1)$, decays with a leading order singularity $\rho_{kink}\propto t^{-1}$ and exhibits a jump at the $p_{in}=0$ axis.

The $N=2$ pair approximation results in the following steady state solution for kinks:

$$\rho_{kink}(\infty)=\frac{4p_{ex}(1-2p_+)p_+}{1+2(4p_{ex}-1)p_+ + 8p_{ex}(2p_{ex}-1)p_+^2}. \qquad (11)$$

This has absorbing states ($\rho_{kink}=0$) along the $p+=0$, $p_{ex}=0$, and $p_+=1/2$ lines and active in the $0<p_+<1/2$, $p_{ex}>0$ region. The transitions, however, are continuous with leading order singularity $\beta=1$ everywhere. As we can see the simple mean-field and higher order cluster-mean-field approximations give different singular behavior similarly to cases treated earlier [25,26,28,29].

For higher order approximations $N>2$, we could only solve the equations for the steady state numerically. We could determine stable solutions up to the $N=6$ level from the coupled nonlinear equations of 36 variables. By locating the phase transition lines we found that the $p_+=0$ and the $p_{ex}=0$ transitions do not change but the $p_+=1/2$ (DP) transition line shifts monotonically towards the $p_+=0$ axis as we increase the level of approximations (see Fig. 2). These solutions converge towards the phase transition line determined by simulations. We found that fairly good quadratic fitting can be applied for the $N=3,4,5,6$ level $p_+^*(p_{ex},N)$ critical point solutions, so we extrapolated to $N\to\infty$ at $p_{ex}=0.1$, 0.3, 0.5, 0.7, and 0.9. The corresponding $p_+^*(p_{ex},\infty)$ curve agrees well with the simulation data (see Table I).

TABLE I. Summary of p_+^* critical point results of $N=3-6$ GMF (generalized mean-field) approximations and simulations.

p_{ex}	$N=3$	$N=4$	$N=5$	$N=6$	$N\to\infty$	MC
0.1	0.419	0.4003	0.3903	0.384	0.357	0.405
0.3	0.3357	0.2963	0.2772	0.2661	0.233	0.272
0.5	0.3000	0.2479	0.2242	0.2111	0.178	0.187
0.7	0.2824	0.2216	0.1945	0.1798	0.146	0.137
0.9	0.2726	0.2057	0.1759	0.1597	0.122	0.107

B. The line of *N*-BARW2 transitions

As we have seen in the preceding section, in the plane of (p_+,p_{ex}) the phase below the phase transition line is the active one and extends down to the $p_{ex}=0$ axis. The critical behavior at and in the neighborhood of this axis has turned out to be of *N*-BARW2 type. In this respect the absorbing states are fully ordered or consist of single $-$ spins performing random walk in the sea of $+$ spins.

The order parameter also in this case is the density of kinks ρ, the steady state value of it disappears when approaching the $p_{ex}=0$ axis as $\rho_\infty \propto p_{ex}^{\beta}$. Simulations from random initial state in a system with size $L=10^5$ were run up to 10^6 MCS. In the supercritical region the steady states have been determined for different p_{ex} values. Following level-off, the densities were averaged over 10^4 MCS and 1000 samples. By looking at the effective exponent defined as

$$\beta_{eff}[p_{ex}(i)] = \frac{\ln \rho_\infty[p_{ex}(i)] - \ln \rho_\infty[p_{ex}(i-1)]}{\ln p_{ex}(i) - \ln p_{ex}(i-1)}, \quad (12)$$

one can read off: $\beta_{eff} \to \beta$. The result of computer simulations at $p_+=0.1$ is shown in Fig. 3. A linear extrapolation for $p_{ex}<0.1$ gives $\beta=1.0\pm.01$. The overshooting of β_{eff} near the critical point is typical in case of logarithmic corrections to scaling. By plotting ρ_∞/p_{ex} as the function of $\ln(p_{ex})$ fairly good linear behavior could be observed in the $0.02<p_{ex}<0.4$ region.

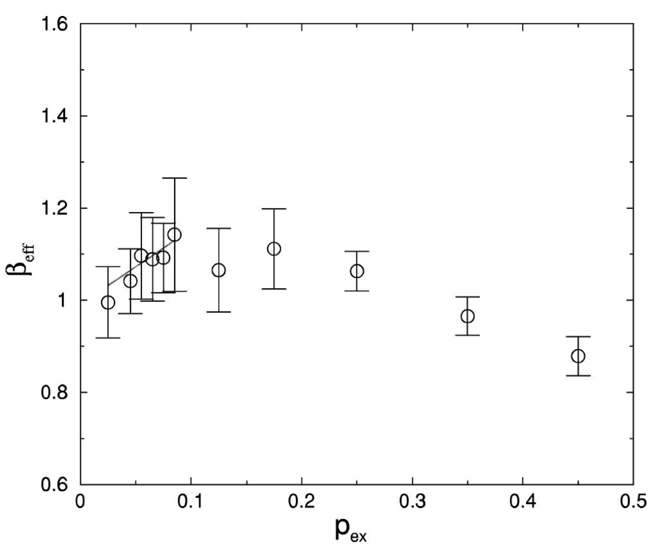

FIG. 3. Effective critical exponent of the order parameter at the $p_{ex}=0$ transition.

TABLE II. Summary of critical exponent estimates at the $p_{ex}=0$ line. The last row shows the data of the 1D *N*-BARW2 class.

p_+	β	α	$\nu_\perp$
0.1	1.00(1)	0.505(5)	1.00(6)
0.4		0.503(5)	
N-BARW2	1	1/2	1

The $\rho(t)$ simulation results at $p_{ex}=0$ and $p_+=0.1,0.4$ were analyzed by the local slopes

$$\alpha_{eff}(t) = \frac{-\ln[\rho(t)/\rho(t/m)]}{\ln(m)} \quad (13)$$

(where $m=8$ is used) (Table II). The asymptotic time evolution of the density of kinks $\rho(t)\sim t^{-\alpha}$ has proven to be, within error, that of annihilating random walk: $\alpha=1/2$ as shown in Fig. 4. A $\sim t^{-0.9}$ correction to scaling gave best fit in both cases. We also tried to fit a logarithmic correction form $\{[a+b\ln(t)]/t\}^{0.5}$ for $\rho(t)$ but b was found to go zero for $t > \sim 6\times 10^5$ MCS in both cases.

As to the remaining critical exponents when approaching $p_{ex}=0$, we checked the expected *N*-BARW2 behavior by measuring the kink density in the active state (steady state) for several small values of p_{ex} (between 0.1 and 0.001) for lattice size L between 50 and 5000. The initial state was prepared in such a way that a cluster of "$-$" spins was chosen of width and location randomly distributed between $L/4$ and $3L/4$. Finite size scaling theory [30] predicts the form

$$\rho(p_{ex},L) = L^{-\beta/\nu_\perp} F(p_{ex} L^{1/\nu_\perp}). \quad (14)$$

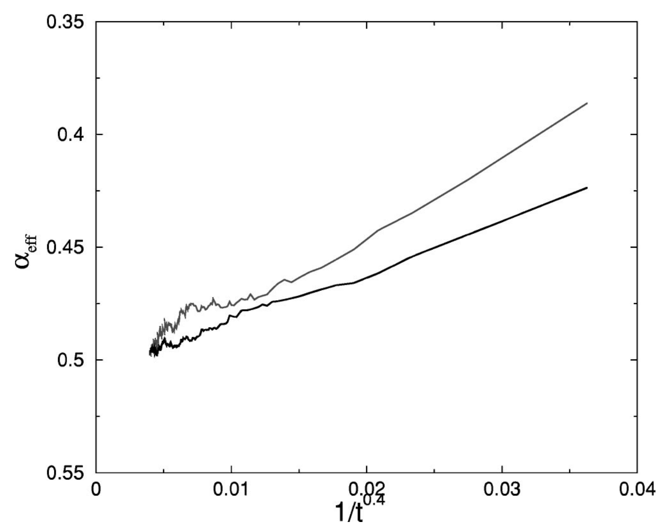

FIG. 4. Effective critical exponent of the kink density at the $p_{ex}=0$, $p_+=0.1$ (lower curve) and $p_+=0.4$ (upper curve) as the function $1/t^{0.4}$. This choice results in a linear plot of the local slopes, corresponding to $\sim t^{-0.9}$ correction to scaling.

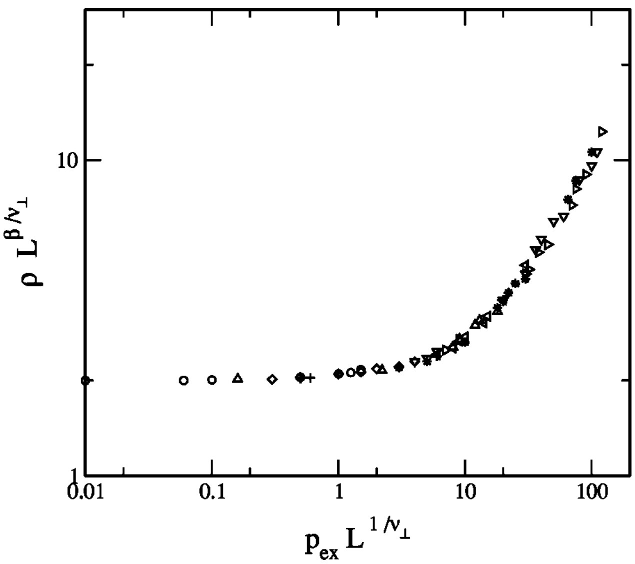

FIG. 5. Data collapse of $\rho L^{\beta/\nu_\perp}$ against $p_{ex}L^{1/\nu_\perp}$ with $\beta/\nu_\perp=1$ for various values of the chain lengths (circle, $L=50$; diamond, $L=100$; plus sign, $L=600$; triangle, $L=800$; triangle left, $L=1000$; star, $L=2000$; triangle right, $L=3000$; triangle down, $L=4000$) on a double logarithmic scale.

Using the value of β as obtained above, we determine $\nu_\perp$ by data collapsing. With $\beta/\nu_\perp=1$ in Fig. 5, we get $\nu_\perp=1.00\pm.06$. Thus our result shows the critical exponent values by Cardy and Täuber [4].

IV. SUMMARY

In this paper, a model has been presented by generalizing the nonequilibrium kinetic Ising model for the case when two kinds of spin anisotropies are present. In addition to the local kinetic bias introduced by Majumdar *et al.* [16] first, by prescribing with probability equal to zero the annihilation of $-$ spins in the neighborhood "$+-+$," we introduce spin anisotropy in the spin-flip rate. Namely, the "$+$" spins are less likely to flip at domain boundaries (with probability p_+) than "$-$" spins (probability 1/2). Branching of kinks (domain boundaries) is the main effect of the spin-exchange part of the model. We have shown by cluster-mean-field calculations and computer simulations that for a given $p_+<1/2$ asymmetry the presence of spin exchange gives rise to two different types of phase transitions. While at $p_{ex}^*=0$ an active phase emerges with a N-BARW2 type of transition, for $p_{ex}^*>0$ this transforms back into an absorbing state with a DP class transition. The spin anisotropies result in a new type of two-component, coupled branching and annihilating random walk of kinks with parity conservation.

At $p_+=1/2$ the MDG point is reached, see Fig. 1. It is the end point of the DP transition line similarly to the compact directed percolation end point of the DP transition line in the Domany-Kinzel cellular automaton model [31]. The absorbing phase is the same in the two models, the active phase, however, is different.

The question arises whether the 1/ln(t) factor in the asymptotic behavior found in Ref. [16] is to be expected to hold even in the present model for $p_{ex}=0$. If this were the case, the N-BARW2 behavior would also be affected. First, from the side of simulations, we have not found any sign of such behavior. Moreover, the physical picture behind the expected asymptotic behavior of spins is also different in the two cases. While MDG argue that at late time the process $-+-\rightarrow-$ with probability unity leads to "$+$" domains sandwiched between much larger "$-$" ones the introduction of the local asymmetric spin-flip magnetic field with bias for "$+$" spins will act against and feed up the "$+$" phase to compensate for their biased annihilation via the MDG process. As a consequence there is no reason to expect a late time logarithmic relaxation of the kink density on the $p_{ex}=0$ line for $p_+<1/2$.

Finally, it is worth noticing that while the PC transition is known to be sensitive to the Z_2 symmetry [14,27] and DP transition appears by destroying it, the N-BARW2 transition seems to be insensitive to this symmetry breaking.

ACKNOWLEDGMENTS

The authors would like to thank the Hungarian research fund OTKA (Grant Nos. T034784, T017493, T025386, and 4012) for support during this study. G. Ódor acknowledges support from the research fund Bolyai (Grant No. BO/00142/99) and from the IKTA project (Project No. 00111/2000). The simulations were performed on the parallel cluster of SZTAKI and on the supercomputer of the NIIF Hungary.

[1] R. J. Glauber, J. Math. Phys. **4**, 191 (1963).
[2] See e.g., K. Kawasaki, *Phase Transitions and Critical Phenomena*, edited by C. Domb and M. S. Green (Academic, New York, 1972), Vol. 2, p. 443.
[3] Z. Rácz, in *Nonequilibrium Statistical Mechanics in One Dimension*, edited by V. Privman (Cambridge University Press, Cambridge, 1996).
[4] J. Cardy and U. Täuber, Phys. Rev. Lett. **77**, 4780 (1996).
[5] P. Grassberger, F. Krause, and T. von der Twer, J. Phys. A **17**, L105 (1984); P. Grassberger, *ibid.* **22**, L1103 (1989).
[6] N. Menyhárd, J. Phys. A **27**, 6139 (1994).
[7] N. Menyhárd and G. Ódor, Braz. J. Phys. **30**, 113 (2000).
[8] H. Takayasu, A. Yu Tretyakov, Phys. Rev. Lett. **68**, 3060 (1992).
[9] I. Jensen, Phys. Rev. E **47**, R1 (1993).
[10] I. Jensen, Phys. Rev. E **50**, 3623 (1994).
[11] D. Zhong and D. ben-Avraham, Phys. Lett. A **209**, 333 (1995).
[12] M. H. Kim and H. Park, Phys. Rev. Lett. **73**, 2579 (1994).
[13] H. Park, M. H. Kim, and H. Park, Phys. Rev. E **52**, 5664 (1995).
[14] H. Park and H. Park, Physica A **221**, 97 (1995).
[15] For a review see, J. Marro and R. Dickman, *Nonequilibrium Phase Transitions in Lattice Models* (Cambridge University

Press, Cambridge, 1996); H. Hinrichsen, Adv. Phys. **49**, 815 (2000).
[16] S. N. Majumdar, D. S. Dean, and P. Grassberger, Phys. Rev. Lett. **86**, 2301 (2001).
[17] S. Kwon, J. Lee, and H. Park, Phys. Rev. Lett. **85**, 1682 (2000).
[18] G. Ódor, Phys. Rev. E **63**, 021113 (2001).
[19] G. Ódor, Phys. Rev. E **63**, 056108 (2001).
[20] G. Ódor, Phys. Rev. E **65**, 026121 (2002).
[21] J. Hooyberghs, E. Carlon, and C. Vanderzande, Phys. Rev. E **64**, 036124 (2001).
[22] G. Ódor and N. Menyhárd, Phys. Rev. E **61**, 6404 (2000).
[23] H. A. Gutowitz, J. D. Victor, and B. W. Knight, Physica D **28**, 18 (1987).
[24] R. Dickman, Phys. Rev. A **38**, 2588 (1988).
[25] G. Ódor and A. Szolnoki, Phys. Rev. E **53**, 2231 (1996).
[26] N. Menyhárd and G. Ódor, J. Phys. A **28**, 4505 (1995).
[27] N. Menyhárd and G. Ódor, J. Phys. A **29**, 7739 (1995).
[28] E. Carlon, M. Henkel, and U. Schollwöck, Phys. Rev. E **63**, 036101 (2001).
[29] G. Ódor, M. C. Marques, and M. A. Santos, Phys. Rev. E **65**, 056113 (2002).
[30] T. Aukrust, D. A. Browne, and I. Webman, Phys. Rev. A **41**, 5294 (1990).
[31] E. Domany and W. Kinzel, Phys. Rev. Lett. **53**, 311 (1984).